20

Mixed Fluids of Water and Carbon Dioxide

Evan Abramson

ABSTRACT

Equations of state, miscibilities, and speciation in mixed fluids of water and carbon dioxide are discussed. A shift in speciation away from solvated molecules of carbon dioxide increases miscibilities. HKF theory as currently formulated is found incapable of properly handling high pressure data, as partial molal volumes asymptote to a constant value with increasing pressure. Current knowledge of the miscibility surface allows an easy quantification of the fractions of water and carbon dioxide loaded into a diamond anvil cell, and thus should facilitate further research into these mixtures.

20.1. INTRODUCTION

Within Earth's crust and mantle, mixed fluids of water and carbon dioxide are agents for metasomatism, induce melting in the surrounding rock, and may be presumed to be important vehicles for carbon transport both within subducting slabs and into and out of the mantle. Beyond the planetary sciences, high-pressure mixtures of these molecules are involved in many industrial concerns, from oil and gas wells (and possible underground carbon sequestration), to supercritical water oxidation, to explosives technology. As well, both water and carbon dioxide are inexpensive and nontoxic solvents; industrial processes may be envisioned that would profit from these desirable traits coupled with the chemical tunability of mixed-solvent properties through variation of pressure, temperature, and mixing ratios.

Models of the mixed fluids inform our understanding of all the above processes. This chapter explores our knowledge of the thermodynamic properties of solutions of water and carbon dioxide at pressures above, roughly, 0.5 GPa, how such properties have been modeled, and how predictions of the models compare with measurements. While applicability to the deep Earth is obvious, even "high pressure" industrial processes are typically undertaken at pressures less than 0.5 GPa, and so it might be thought that a study restricted to conditions above this limit would be irrelevant to industry. However, desired thermodynamic data often do not exist at pressures intermediate between a few MPa and those considered here, and extrapolations into this range, from lower pressure data, can be erroneous. Interpolations, on the other hand, between the data more easily obtained at a few MPa and and those available above 0.5 GPa may produce useful predictions of properties at the desired intermediate pressures.

20.2. AVAILABLE DATA

Mixtures of water and carbon dioxide have been extensively investigated up to pressures of several hundred MPa, with experimental results considerably less available at the higher pressures considered here (see compilations in Duan & Zhang, 2006; Gernert & Span, 2016; Mader, 1991). Data include direct measurements of molar volume, miscibilities, conditions of chemical equilibria with thermodynamically characterized solids, and spectroscopic observations of speciation. Additionally, computer simulations have been used to predict both equations of state (EOS) and speciation (Brodholt & Wood, 1993; Duan & Zhang, 2006; Fu et al., 2017; Pan &

Department of Earth and Space Sciences, University of Washington, Seattle, Washington, USA

Carbon in Earth's Interior, Geophysical Monograph 249, First Edition. Edited by Craig E. Manning, Jung-Fu Lin, and Wendy L. Mao.

Galli, 2016). Only at quite low pressures, <30 MPa, have specific heats and enthalpies of mixing been reported. Regions in which higher pressure (experimental) data are available are shown in Figure 20.1. With the exception of the rectangle at lowest pressures, each of the depicted regions derives from a single study.

Of particular note are two studies of synthetic inclusions, that of Sterner and Bodnar (1991), up to 0.6 GPa and from 400 °C to 700 °C taken in a quartz host, and of Frost and Wood (1997), between 1 and 2 GPa and from 1100 °C to 1400 °C taken in corundum. Both indicate that excess volumes of mixing are positive and small (<4%), within the explored ranges of pressure and temperature. Volumes deduced from inclusions are uncertain by roughly 1%–2%, only slightly less than the reported excess volumes of mixing, but as pointed out, "The relative incompressibility … at high pressure (high density) tends to magnify the effect of even subtle non-ideal behavior" (Sterner & Bodnar, 1991).

Chemical potentials have been determined directly from observations of chemical equilibria involving the carboxylation/decarboxylation or hydration/dehydration of various minerals in contact with solutions of defined mole fraction CO_2 (XCO_2). Such experiments have been run at temperatures as low as 310 °C and up to 1200 °C; pressures have typically not exceeded 0.6 GPa, although a few measurements have been made at substantially higher pressures. In particular, Aranovitch and Newton (1999) observed both decarboxylation and dehydration reactions of silicate minerals at pressures up to 1.4 GPa and from 600 °C to 1100 °C, while Eggler et al. (1979) reported on a decarboxylation reaction at 2.6 GPa and 1100 °C.

Speeds of sound in mixed solutions have more recently been measured in a high-pressure diamond anvil cell (DAC) by Brillouin spectroscopy (Qin et al., 2010) and by impulsively stimulated scattering (Abramson, unpublished). A set of such measurements, accurate over a broad range of P and T, would be extremely useful. Unfortunately, at the temperatures of interest, pressure gauges of the usual kind either dissolve, have a poor (e.g., ±0.1 GPa) precision, or both. Thus, the data taken in these preliminary experiments are not likely to be useful.

Observations of miscibility and of speciation taken in the DAC are also included in Figure 20.1, and will be discussed below. What is apparent from this initial diagram, however, is that information relevant to the nature of the CO_2/H_2O fluid above pressures of half a GPa are few, span two separate ranges of pressure and temperature, and that these two ranges comprise quite different types of data. For this reason, the situation has not been greatly advanced since 1991, when Mader wrote, "It is concluded that the data-base available is not yet adequate to derive a reliable equation of state for H_2O-CO_2 mixtures."

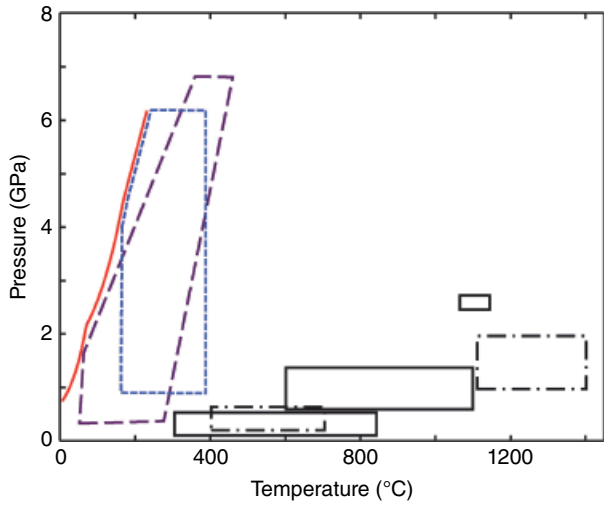

Figure 20.1 Pressure-temperature regions of published H_2O/CO_2 data extending to higher pressures. Miscibility data, long dashed lines, are limited at higher temperatures by the critical curve (Abramson et al., 2017a); speciation, short dashed lines; volume by inclusions, dot-dash (Frost & Wood, 1997, Sterner & Bodnar, 1991); dehydration or decarboxylation equilibria, solid lines (Aranovitch & Newton,1999; Eggler et al., 1979, and others listed in the compilation of Mader, 1991). The solid curve at lower temperatures demarks the solidus (Abramson, 2017; Abramson et al., 2017b). See electronic version for color representation of the figures in this book.

20.3. MISCIBILITIES

A basic question to be asked about the nature of these fluids is, to what degree are water and carbon dioxide miscible at any given pressure and temperature? Until recently, the miscibility surface of this binary had been studied to a maximum pressure of 0.35 GPa (Mather & Franck, 1992; Sterner & Bodnar, 1991; Takenouchi & Kennedy, 1964; Todheide & Franck, 1963). Both Todheide and Franck (1963) and Takenouchi and Kennedy (1964) made direct measurements of the contents of coexisting phases, while Mather and Franck (1992) measured pressures and temperatures of homogenization for (three) samples of known contents, and Sterner and Bodnar (1991) inferred the same from the use of synthetic fluid inclusions. As seen in Figure 20.2, the critical curve descends in temperature from the critical point of pure water, 374 °C (at 22 MPa), to a minimum at roughly 266 °C (at 0.245 GPa) before beginning to rise again with further increase in pressure; the associated critical concentration at the saddle point is around XCO_2 = 42%. The values given in the preceding sentence are those from Todheide and Franck (1963), but though the four works are in loose agreement over the breadth of the measurements, they can still differ considerably, particularly in the region of high XCO_2. For example, in the two-fluid regime at 0.20 GPa and 260 °C, XCO_2 for the carbonic fluid is given as 47%, 57%, 63%, or 66%.

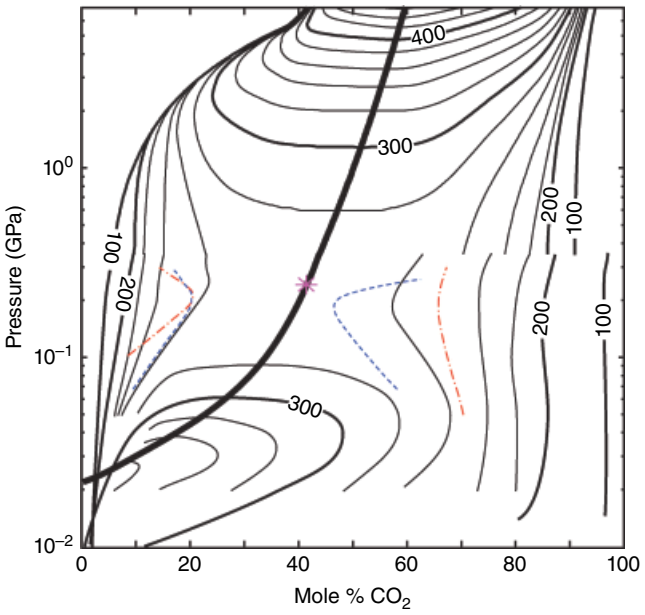

Figure 20.2 Miscibility surface, plotted against mole fraction carbon dioxide and pressure (Abramson et al., 2017a); contours of temperature (°C) are given in 20 °C intervals. Below 0.35 GPa, curves derive from data of Todheide and Franck (1963). The thick line indicates the critical curve, with an asterisk denoting the saddle point. For comparison, the 260° contours from the works of Takenouchi and Kennedy (1964) (dashed lines) and of Sterner and Bodnar (1991)(dot and dash) are also shown (the study of Mather and Frank (1992) comprises only three isopleths, insufficient to define a surface). See electronic version for color representation of the figures in this book.

Abramson et al. (2017a) have now measured miscibilities of water–carbon dioxide mixtures, up to a pressure of 7 GPa, through the visual observation of homogenization (mixing) within a DAC. In these experiments, the cell contents were loaded as two separate fluids, the resulting XCO_2 being determined through isotopic doping of the water and subsequent measurement of the amount transferred to the CO_2. These studies are limited to pressures in excess of 0.4 GPa and thus do not overlap those previously cited, although they are in rough agreement with the results of Todheide and Franck (1963). Even with these new results, the critical curve continues to rise to the highest pressure and temperature of the experiments; the conditions under which two immiscible fluids can coexist thus extend yet higher, into unexplored regions.

An interesting feature of the data is the area of closely spaced contours above the saddle-point and centered around XCO_2 = 30%. In this region, an isothermal increase of pressure (e.g. applied to a fluid of XCO_2 = 30%, held at 300 °C, starting at 1 GPa) causes a homogeneous solution first to unmix, then to remix. The initial unmixing was the expected behavior for pressures exceeding that of the saddle-point. The remixing, seen so far only for XCO_2 < 40%, coincides with, and is presumably due to, a pressure-induced shift in speciation.

20.4. SPECIATION

At lower pressures, CO_2 exists as the solvated molecule, CO_2(aq). However, in Raman spectra taken at the higher pressures attained with the DAC (Abramson et al., 2017a), lines associated with CO_2(aq) disappear, to be replaced with a new line, hypothesized to be due to the carbonic acid molecule (Wang et al., 2016), but more likely to represent the appearance of the bicarbonate ion. The widely used Helgeson-Kirkham-Flowers (HKF) formalism (Helgeson et al., 1981) for solutes in aqueous solution, as revised by Shock et al. (1992), can be used to approximate the CO_2(aq)-HCO_3^{-1} equilibrium with results as seen in Figure 20.3. These calculations are necessarily approximate; the required thermodynamic parameters (Facq et al., 2014) for bicarbonate are supported by the bicarbonate-carbonate equilibrium observed at comparable pressure and temperature, but those pertaining to CO_2(aq) only by data at pressures <35 MPa. Additionally, the dielectric constant was taken to be that of pure water, and no attempt was made to calculate activity coefficients for a solution containing 17 mol% CO_2 (which coefficients were assumed to be 1, as for a dilute solution). Even so, the calculated pressures for equimolar solutions, while higher than those measured, are still within a few GPa, and are consistent with the hypothesis that the new species is bicarbonate rather than carbonic acid; data that would allow the corresponding calculation for carbonic acid do not exist. Guidance from theoretical calculations is available only from the work of Pan and Galli (2016), who have used molecular dynamics based on density functional theory to investigate speciation in a dilute (XCO_2 = 1.6%) solution at 11 GPa and 1000 K. Their results show, as expected, no CO_2(aq) to be present, with roughly 80% of the carbon existing as bicarbonate, and the balance either of equal amounts of carbonate and carbonic acid, or mostly carbonic acid, depending on the functional chosen to represent the exchange correlation.

From Figure 20.3, we see that the reaction of CO_2(aq) to form the new species is favored by increasing pressure and decreasing temperature, in accord with the HKF calculations for bicarbonate. The data of Facq et al. (2014) also show, similarly, that higher pressures favor deprotonation of bicarbonate to yield carbonate, while higher temperatures result in the reverse. HKF, however, did not reproduce the observed miscibility equilibrium of fluid carbon dioxide, CO_2(f), with CO_2(aq). Up to roughly 1 GPa experimental data are qualitatively reproduced as pressure rises, with CO_2 first forced into solution and

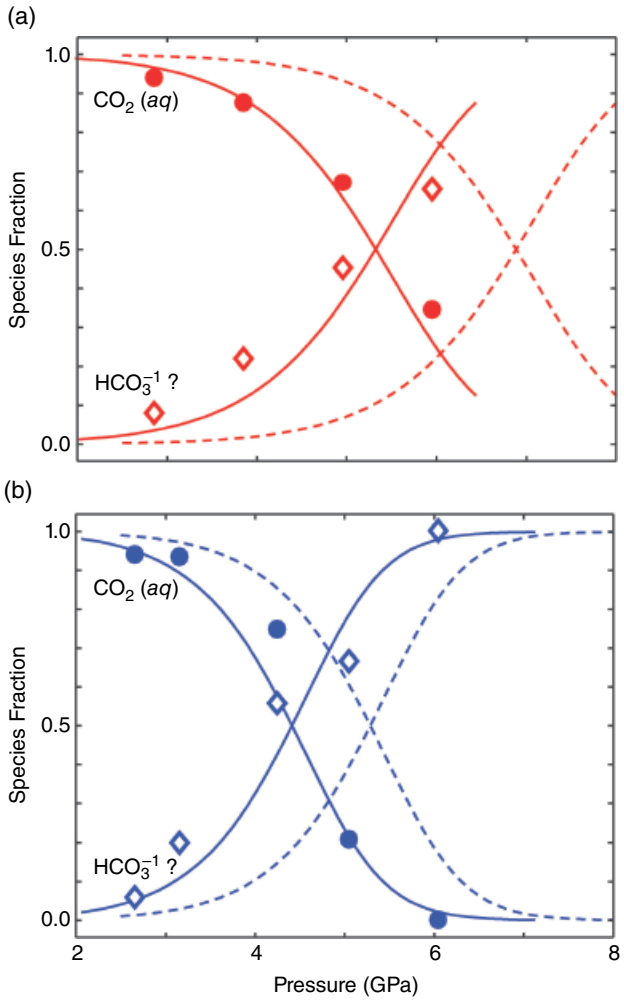

Figure 20.3 Fraction of CO_2 dissolved as the solvated molecule (filled circles) or, probably, bicarbonate (diamonds) as measured from Raman spectra of a solution with 17 mol% CO_2, and at temperatures of (a) 400 °C and (b) 300 °C. Solid lines are drawn through the data. Dashed lines indicate calculations based on the assumption that the higher pressure species is the bicarbonate ion, and use of the parameters given in Facq et al. (2014). See electronic version for color representation of the figures in this book.

then, with further increase in pressure, progressive unmixing. However, as pressure continues to rise, the experimentally observed remixing is not predicted, even while the concentration of CO_2(aq) is predicted (and seen) to diminish in favor of the bicarbonate species.

This divergence of experiment and theory was caused by the use of the current HKF formalism for the solutes in conjunction with experimentally determined fluid volumes for CO_2(f). Within the formalism, partial molar volumes at infinite dilution, V^0, are given by an expression that rapidly asymptotes to a constant value as pressure increases. The formula, developed for lower pressure work, thus results in a V^0 with an unphysical lower limit. Shown in Figure 20.4 are the predicted volumes of both CO_2(aq) and bicarbonate ion, as well as the experimentally determined values for pure CO_2 fluid. The solvated molecule upon compression is calculated to approach a limiting value of ~33 cm³/mol. The volume of the bicarbonate ion actually increases due to a diminution of the electrostrictive effect (as the compressibility of water also diminishes), but it too is predicted to reach a limiting value, of ~32 cm³/mol. In contrast, and as expected, the measured volume of CO_2(f) decreases without apparent limit. The result is that there will always be a pressure high enough that the increases of chemical potential, calculated for both aqueous species as $\int V^0 dP$, exceed that of the pure fluid, resulting in the incorrect prediction that the system will remain unmixed.

In contrast, recent analyses (Brown et al., 2018) of solution data indicate that at pressures near 1 GPa, partial volumes of a solute will approach that of the pure substance (for the same pressure and temperature). Partial volumes of CO_2(aq) and HCO_3^{-1} might then be expected to approximate to those of the pure fluid CO_2 rather than the behavior depicted in Figure 20.4. Although the current formalism can be forced to represent high pressure data (e.g. in Facq et al., 2014), any close fit to observed equilibria is presumably due to compensating errors and should not be expected to remain useful to higher pressures or in conjunction with experimentally derived volumes.

20.5. EQUATION OF STATE

Several equations of state of the binary mixture, taken from the literature (Aranovich & Newton, 1999; Holland & Powell, 2003; Kerrick & Jacobs, 1981; Zhang & Duan, 2010), have been tested against the miscibility surface (Abramson et al., 2017a). Measured and predicted critical curves are shown in Figure 20.5. Three of these EOS were based entirely on the measurements available at relatively low pressures and high temperatures, while Zhang and Duan (2010) supplemented data with molecular dynamic calculations up to 10 GPa, but with the assumption that the carbon dioxide continues to exist as the solvated molecule. Given the large disparity in the pressure-temperature region from which data in support of the various EOS derive, and the region of the miscibility surface where the EOS are being tested (see Figure 20.1), it is surprising that the predictions are even as close to experimental measurements as seen. The EOS of Holland and Powell (2003), for instance, relies on only a single, free fitting parameter for a small excess Gibbs energy and yet parallels (roughly) the observed critical curve.

For all four EOS, the experimentally determined two-phase region lies at higher pressures than predicted. It is

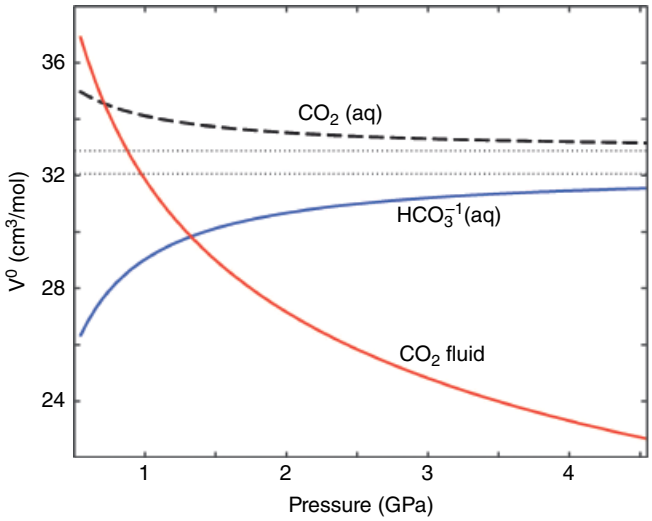

Figure 20.4 Partial molal volumes at infinite dilution, V^0, of solvated CO_2 and bicarbonate ion as calculated, as well as measured volumes of fluid CO_2 (Giordano et al., 2006), are plotted against pressure for a temperature of 300 °C. Dotted lines indicate asymptotes. See electronic version for color representation of the figures in this book.

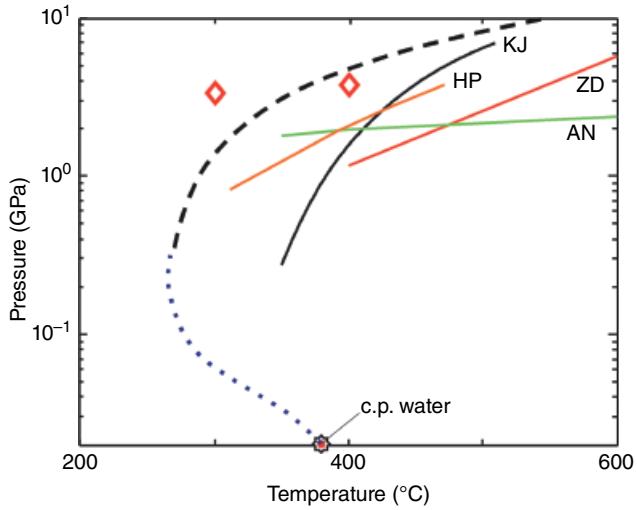

Figure 20.5 Critical pressures are plotted against temperature. Experimental data are from Todheide and Franck (1963) (dots) and Abramson et al. (2017a) (dashes); the critical point of pure water is also indicated. Predictions of four EOS are shown: Kerrick and Jacobs, 1981; Aranovich and Newton, 1999; Holland & Powell, 2003; Zhang & Duan, 2010. The two diamonds indicate points at which rising pressure has resulted in the conversion of roughly 20% of dissolved carbon dioxide from CO_2(aq) to another species (in a solution of $XCO_2 = 17\%$). See electronic version for color representation of the figures in this book.

interesting to speculate as to whether this commonality is due to the observed shift in speciation, which might be expected to delay the onset of unmixing with rising pressure. The two diamonds drawn in the figure indicate where, in the data of Figure 20.3, the fraction of carbon dioxide existing as CO_2(aq) has been reduced by 20%, and might be taken to roughly indicate where the new species begins to significantly affect the EOS. Thus, the nature of the EOS may approximate to an ideal mixing at lower pressures, but less so at higher pressures due to an altered speciation.

20.6. AVENUES FOR PROGRESS

Experiments in the high-pressure DAC require a means of quantifying the fractions of the two independently loaded components. Values of the loaded XCO_2 can be estimated by a visual determination of the relative volumes of the immiscible phases (Qin, 2010); however, the accuracy of this method is dubious. In Abramson et al. (2017a), water was isotopically doped, and subsequent isotopic transfer within the DAC allowed proportions to be determined to ~3% absolute. The process, which is both laborious and time consuming, can only be performed after the end of the main experiment as it requires transferring contents of the DAC into a mass spectrometer. Fortunately, now that the miscibility has been mapped out, the contents of a DAC can be evaluated over much of the possible range of XCO_2 by comparison of the observed fluid-fluid mixing with the miscibility surface; this should facilitate further research on speciation in the binary. Of course, the same comparison might also be used to define CO_2/H_2O ratios in systems with additional components (e.g. SiO_2) as long as they do not dissolve appreciably at the lower temperatures of mixing.

As mentioned earlier, an (accurate) evaluation of speeds of sound would be very useful. Given the ability to

determine XCO_2 from observations of mixing and unmixing, it may now be possible to use the divided cell method in the DAC (Abramson & Brown, 2004) with the relatively accurate (but, unfortunately, water soluble) $(Sm)SrB_4O_7$ pressure gauge, and either Brillouin spectroscopy or impulsively stimulated scattering. Traditional acoustic techniques may also be applied in large-volume presses (Song et al., 2011).

ACKNOWLEDGMENTS

This text was prepared with partial funding from National Science Foundation grant EAR-1829147.

REFERENCES

Abramson, E. H. (2017). Three-phase melting curves in the binary system of carbon dioxide and water. *Journal of Physics: Conference Series*, *950*, 042019. https://doi.org/10.1088/1742-6596/950/4/042019

Abramson, E. H., Bollengier, O., & Brown, J. M. (2017a). The water-carbon dioxide miscibility surface to 450 °C and 7 GPa. *American Journal of Science*, *317*, 967–989, https://doi.org/10.2475/09.2017.01

Abramson, E. H., Bollengier, O., & Brown, J. M. (2017b). Water-carbon dioxide solid phase equilibria at pressures above 4 GPa. *Scientific Reports*, *7*, 821. https://doi.org/10.1038/s41598-017-00915-0

Abramson, E. H., & Brown, J. M. (2004). Equation of state of water based on speeds of sound measured in the diamond-anvil cell. *Geochimica et Cosmochimica Acta*, *68*, 1827–1835. https://doi.org/10.1016/j.gca.2003.10.020

Aranovich, L. Y., & Newton, R. C. (1999). Experimental determination of CO_2-H_2O activity-composition relations at 600–1000 °C and 6–14 kbar by reversed decarbonation and dehydration reactions. *American Mineralogist*, *84*, 1319–1332.

Brodholt, J., & Wood, B. (1993). Molecular dynamics simulations of the properties of CO_2-H_2O mixtures at high pressures and temperatures. *American Mineralogist*, *78*, 558–564.

Brown, J. M., Bollengier, O., & Vance, S. (2018). *High-Pressure "Death" of Aqueous Electrolytic Chemistry*. Paper presented at WaterX Exotic Properties of Water under Extreme Conditions, Water X International workshop, La Maddalena, Sardinia (Italy).

Duan, Z., & Zhang, Z. (2006). Equation of state of the H_2O, CO_2, and H_2O–CO_2 systems up to 10 GPa and 2573.15 K: Molecular dynamics simulations with ab initio potential surface. *Geochimica et Cosmochimica Acta*, *70*, 2311–2324.

Eggler, D. H., Kushiro, I., & Holloway, J. R. (1979). Free energies of decarbonation reactions at mantle pressures: I. Stability of the assemblage forsterite-enstatite-mangesite in the system MgO-SiO_2-CO_2-H_2O to 60 kbar. *American Mineralogist*, *64*, 288–293.

Facq, S., Daniel, I., Montagnac, G., Cardon, H., & Sverjensky, D. A. (2014). In situ Raman study and thermodynamic model of aqueous carbonate speciation in equilibrium with aragonite under subduction zone conditions. *Geochimica et Cosmochimica Acta*, *132*, 375–390.

Frost, D. J., & Wood, B. J. (1997). Experimental measurements of the properties of H_20-CO_2 mixtures at high pressures and temperatures. *Geochimica et Cosmochimica Acta*, *61*, 3301–3309.

Fu, J., Zhao, J., Plyasunov, A. B, & Belonoshko, A. B. (2017). Ab initio molecular dynamics study of fluid H_2O-CO_2 mixture in broad pressure-temperature range. *AIP Advances*, *7*, 115217. https://doi.org/10.1063/1.5006131

Gernert, J., & Span, R. (2016). EOS–CG: A Helmholtz energy mixture model for humid gases and CCS gases and CCS mixtures. *The Journal of Chemical Thermodynamics*, *93*, 274–293.

Giordano, V. M., Datchi, F., & Dewaele, A. (2006) Melting curve and fluid equation of state of carbon dioxide at high pressure and high temperature. *The Journal of Chemical Physics*, *125*, 054504.

Helgeson, H. C., Kirkham, D. H., & Flowers, G. C. (1981). Theoretical predictions of the thermodynamic behavior of aqueous electrolytes at high pressures and temperatures: IV. Calculation of activity coefficients, osmotic coefficients, and apparent molal and standard and relative partial molal properties to 600 °C and 5Kb, *American Journal of Science*, *28*, 1249–1516.

Holland, T., & Powell, R. (2003). Activity–composition relations for phases in petrological calculations: An asymmetric multicomponent formulation. *Contributions to Mineralogy and Petrology*, *145*, 492–501.

Kerrick, D. M., & Jacobs, G. K. (1981). A modified Redlich-Kwong equation for H2O, CO2, and H2O–CO2 mixtures at elevated pressures and temperatures. *American Journal of Science*, *281*(6), 735–767. https://doi.org/10.2475/ajs.281.6.735

Mader, U. K. (1991). H_2O-CO_2 mixtures: A review of P-V-T-X data and an assessment from a phase-equilibrium point of view. *Canadian Mineralogist*, *29*, 767–790.

Mather, A. E., & Franck, E. U. (1992). Phase equilibria in the system carbon dioxide-water at elevated pressures. *The Journal of Physical Chemistry*, *96*, 6–8.

Pan, D., & Galli, G. A. (2016). The fate of carbon dioxide in water-rich fluids under extreme conditions. *Science Advances*, *2*, e1601278.

Qin, J., Li, M., Li, J., Chen, R., & Duan, Z. (2010). High temperatures and high pressures Brillouin scattering studies of liquid H2O+CO2 mixtures. *The Journal of Chemical Physics*, *133*, 154513. https://doi.org/10.1063/1.3495972

Shock E. L., Oelkers, E. H., Johnson, J. W., Sverjensky, D. A., & Helgeson, H. C. (1992). Calculation of the thermodynamic properties of aqueous species at high pressures and temperatures: Effective electrostatic radii, dissociation constants and standard partial molal properties to 1000 °C and 5 kbar. *Journal of the Chemical Society, Faraday Transactions*, *88*, 803–826.

Song, W., Liu, Y., Wang, Z., Gong, C., Guo, J., Zhou, W., & Xie, H. (2011). Measurement method for sound velocity of melts in large volume press and its application to liquid sodium up to 2.0 GPa. *Review of Scientific Instruments*, *82*, 086108. https://doi.org/10.1063/1.3625267

Sterner, S. M., & Bodnar, R. J. (1991). Synthetic fluid inclusions. X: Experimental determination of P-V-T-X properties in the CO_2-H_2O system to 6 kb and 700 °C. *American Journal of Science*, *291*, 1–54.

Takenouchi, S., & Kennedy, G. C. (1964). The binary system CO_2-H_2O at high temperatures and pressures. *American Journal of Science*, *262*, 1055–1074.

Todheide, K., & Franck, E. U. (1963). Das Zweiphasengebiet und die Kritische Kurve in System Kohlendioxide-Wasser bis zu Drucken von 3500 Bar. *Zeitschrift fuer Physikalische Chemie (Neue Folge)*, *37*, 387–401.

Wang, H., Zeuschner, J., Eremets, M., Troyan, I., & Willams, J. (2016). Stable solid and aqueous H_2CO_3 from CO_2 and H_2O at high pressure and high temperature. *Scientific Reports*, *6*, 19902.

Zhang, C., & Duan, Z. (2010). GFluid: An Excel spreadsheet for investigating C–O–H fluid composition under high temperatures and pressures. *Computers and Geosciences*, *36*, 569–572.